0022-3565/11/3363-652–660$20.00
THE JOURNAL OF PHARMACOLOGY AND EXPERIMENTAL THERAPEUTICS
JPET 336:652–660, 2011

Vol. 336, No. 3
175331/3668440
Printed in U.S.A.

ELR510444, A Novel Microtubule Disruptor with Multiple Mechanisms of Action

A. L. Risinger, C. D. Westbrook, A. Encinas, M. Mülbaier, C. M. Schultes, S. Wawro, J. D. Lewis, B. Janssen, F. J. Giles, and S. L. Mooberry

Department of Pharmacology, University of Texas Health Science Center at San Antonio, San Antonio, Texas (A.L.R., C.D.W., S.L.M.); ELARA Pharmaceuticals GmbH, Heidelberg, Germany (A.E., M.M., C.M.S., S.W., J.D.L., B.J.); and Department of Medicine, University of Texas Health Science Center at San Antonio, San Antonio, Texas (F.J.G., S.L.M.)

Received September 21, 2010; accepted December 8, 2010

ABSTRACT

Although several microtubule-targeting drugs are in clinical use, there remains a need to identify novel agents that can overcome the limitations of current therapies, including acquired and innate drug resistance and undesired side effects. In this study, we show that ELR510444 has potent microtubule-disrupting activity, causing a loss of cellular microtubules and the formation of aberrant mitotic spindles and leading to mitotic arrest and apoptosis of cancer cells. ELR510444 potently inhibited cell proliferation with an IC_{50} value of 30.9 nM in MDA-MB-231 cells, inhibited the rate and extent of purified tubulin assembly, and displaced colchicine from tubulin, indicating that the drug directly interacts with tubulin at the colchicine-binding site. ELR510444 is not a substrate for the P-glycoprotein drug transporter and retains activity in βIII-tubulin-overexpressing cell lines, suggesting that it circumvents both clinically relevant mechanisms of drug resistance to this class of agents. Our data show a close correlation between the concentration of ELR510444 required for inhibition of cellular proliferation and that required to cause significant loss of cellular microtubule density, consistent with its activity as a microtubule depolymerizer. ELR510444 also shows potent antitumor activity in the MDA-MB-231 xenograft model with at least a 2-fold therapeutic window. Studies in tumor endothelial cells show that a low concentration of ELR510444 (30 nM) rapidly alters endothelial cell shape, similar to the effect of the vascular disrupting agent combretastatin A4. These results suggest that ELR510444 is a novel microtubule-disrupting agent with potential antivascular effects and in vivo antitumor efficacy.

Introduction

Microtubule-targeting agents are some of the most effective chemotherapeutic agents used in the clinic today. These drugs are often divided into two categories: microtubule stabilizers, which include the taxanes and epothilones, and microtubule depolymerizers, which include the vinca alkaloids and colchicine site agents. Although these two classes are differentiated by their effects on interphase microtubules, all microtubule-active drugs effectively kill cancer cells through a common mechanism of inhibiting microtubule dynamics, leading to mitotic defects and subsequent apoptosis (Jordan and Kamath, 2007).

Microtubule destabilizers currently in clinical use include the vinca alkaloids vinblastine, vincristine, and vinorelbine, which all bind to what has been termed the "vinca site" on tubulin. Other agents that bind within this site, including vinflunine and the halichondrin derivative eribulin (E7389; Halaven), are undergoing clinical trials in a number of solid tumor types. The other recognized binding site for microtubule-destabilizing agents is the colchicine-binding site. Although colchicine is not used as an anticancer agent because of its unacceptable toxicity, there have been multiple efforts to clinically develop colchicine site drugs with more favorable toxicity profiles. 2-Methoxyestradiol was one colchicine site agent that was evaluated clinically and had an acceptable toxicity profile, but it failed to advance to US Food and Drug Administration approval because of its low efficacy (Rajku-

This work was supported by the National Institutes of Health National Cancer Institute Cancer Therapy and Research Center [Grant CA054174], the President's Council Excellence Award (to S.L.M.), and the Department of Defense Congressionally Directed Medical Research Programs Postdoctoral Award [BC087466] (to A.L.R.). Research at ELARA was partly funded through the Bundesministerium für Bildung und Forschung GO-Bio program Förderkennzeichen 0315418 ("Optimization and Preclinical Development of Small Molecule Therapeutics with Unique Mechanisms of Action in Cancer") and Excellence Cluster initiative Förderkennzeichen 01EX0817 ("Spitzencluster BioRN, Verbundprojekt Inkubator: BioRN-INA-TP04").

Article, publication date, and citation information can be found at http://jpet.aspetjournals.org.

doi:10.1124/jpet.110.175331.

ABBREVIATIONS: E7389, eribulin; Pgp, P-glycoprotein; VDA, vascular disrupting agent; CA-4, combretastatin A4; ABT-751, *N*-[2-[(4-hydroxyphenyl)amino]-3-pyridinyl]-4-methoxybenzenesulfonamide; FBS, fetal bovine serum; SRB, sulforhodamine B; Rr, relative resistance; MDR1, multidrug resistance 1; MDCK, Madin-Darby canine kidney; DAPI, 4,6-diamidino-2-phenylindole; DMSO, dimethyl sulfoxide; BW, body weight.

mar et al., 2007). More metabolically stable 2-methoxyestradiol analogs are now being studied (Pasquier et al., 2010).

One drawback of microtubule-targeting agents is innate and acquired drug resistance. The most common form of clinical resistance to microtubule-targeting agents is overexpression of the *MDR1* gene, which encodes the P-glycoprotein (Pgp) drug efflux pump (Fojo and Menefee, 2007). The innate expression of this efflux pump in tissues, including those of the liver, kidney, and gastrointestinal tract, limits the accumulation and thereby the cytotoxic activity of drugs that are Pgp substrates (Leonard et al., 2003). In addition, expression of Pgp is associated with poor response to microtubule-targeted agents and subsequent treatment failure (Trock et al., 1997; Chiou et al., 2003). The other clinically relevant form of resistance to microtubule-targeting agents is overexpression of the βIII isotype of tubulin (Sève and Dumontet, 2008). Therefore, the clinical development of a microtubule-targeting agent that circumvents both of these mechanisms of drug resistance could have advantages for patients with drug-resistant tumors.

The most widely studied class of colchicine site agents currently in clinical development are the combretastatins, which include combretastatin A4 phosphate (Zybrestat; OXiGENE, South San Francisco, CA) and combretastatin A1 phosphate (OXi4503; OXiGENE). These agents are phosphate prodrugs that increase the aqueous solubility of the naturally occurring combretastatins A4 and A1. In addition to their direct effects on cancer cells, the combretastatins have demonstrated the ability to rapidly destroy tumor vasculature, causing a dramatic decrease in perfusion and leading to central tumor necrosis (Kanthou and Tozer, 2009). Although this diminishes tumor burden, a rim of viable cancer cells remain at the tumor periphery, leading to tumor regrowth. Evidence suggests that vascular disrupting agents (VDAs), which include the combretastatins, may be most effective when used in combination with conventional chemotherapeutic agents, radiation, or antiangiogenic agents that can target the remaining viable rim of tumor cells (Horsman and Siemann, 2006). Clinical and preclinical studies exploring the efficacy of these combinations are an active area of research, including optimization of the timing and dosing of these agents to maximize their antivascular and antimitotic properties (Gridelli et al., 2009).

Materials and Methods

Materials. Combretastatin A4 (CA-4) hydrochloride was obtained from the Drug Synthesis and Chemistry Branch, Developmental Therapeutics Program, Division of Cancer Treatment and Diagnosis, National Cancer Institute (Bethesda, MD). Propranolol, prazosin, cyclosporin, and paclitaxel were purchased from Sigma-Aldrich (St. Louis, MO). ELR510444 was synthesized by ELARA Pharmaceuticals, and ABT-751 (Yoshimatsu et al., 1997) was obtained from Maybridge Chemicals (Trevillet, UK). Colchicine was kindly provided by Milton Brown (Lombardi Cancer Center, Georgetown University, Washington, DC).

Cell Culture. MDA-MB-231 breast cancer cells, HeLa cervical cancer cells, SK-OV-3 ovarian cancer cells, A10 embryonic rat aortic smooth muscle cells, and 2H-11 murine tumor endothelial cells were purchased from American Type Culture Collection (Manassas, VA). The MDA-MB-435 human melanoma cancer cell line was obtained from the Lombardi Cancer Center. CellSensor HRE-*bla* HCT-116 cells were obtained from Invitrogen (Carlsbad, CA). A single-cell clone from transfection of HeLa cells with βIII-tubulin, designated WTβIII, was constructed and maintained as described previously (Joe et al., 2008). A single-cell clone from transduction of SK-OV-3 cells with the *MDR1* gene, designated SK-OV-3/MDR-1-6/6, was generated as described previously (Risinger et al., 2008). MDA-MB-231 and MDA-MB-435 cells were cultured in Richter's improved minimal essential medium (Invitrogen) with 10% FBS and 25 μg/ml gentamicin. HeLa, WTβIII, SK-OV-3, SK-OV-3/MDR-1-6/6, and A10 cells were cultured in basal medium Eagle (Sigma-Aldrich) with 10% FBS and 50 μg/ml gentamicin. 2H-11 cells were cultured in Dulbecco's modified Eagle's medium (Invitrogen) with 10% FBS and 50 μg/ml gentamicin. The CellSensor HRE-*bla* HCT-116 cell line was grown in McCoy's 5A medium supplemented with 10% FBS, penicillin/streptomycin, and 5 μg/ml blasticidin as a selection marker. To ensure the quality and consistency of our cell lines over time, we run full-dose response curves and calculate IC_{50} values for known compounds such as paclitaxel or CA-4 when evaluating experimental compounds. In addition, we evaluate the cell cycle profiles of our cells by flow cytometry on a regular basis to ensure that the cell line is not accumulating aneuploid or octoploid populations and that the cells respond to paclitaxel with full arrest in G_2/M at the appropriate concentration for each line. In addition, we bring up fresh cells every 6 months regardless of whether they pass these experimental checkpoints.

Inhibition of Cellular Proliferation. The SRB assay was used to determine the IC_{50} for inhibition of proliferation (Skehan et al., 1990) as previously described (Tinley et al., 2003b). In brief, cells were plated in 96-well plates, and compounds were added 24 h later. After 48 h of drug exposure, cells were fixed with trichloroacetic acid and stained with SRB dye. Cell density was determined by the absorbance of the SRB solution at A_{560}. The average percent inhibition of cell proliferation ± S.D. was determined for each concentration in at least three independent experiments, each performed in triplicate. The IC_{50} value for inhibition of cellular proliferation ± S.D. was determined from the linear portion of the log dose-response curve from three to four independent experiments using regression analysis. The relative resistance (Rr) values for each drug were calculated by dividing the IC_{50} of the resistant cell line by the IC_{50} of the respective parental cell line.

MDR1-MDCK Permeability Assay. The ability of drugs to be transported by the Pgp drug efflux transporter was determined using Cyprotex's MDR1-MDCK permeability assay (see http://www.cyprotex.com/product_sheets/Cloe%20Screen%20MDR1-MDCK%20Permeability%20(P-glycoprotein)%20Product%20Sheet.pdf). In brief, MDCK cells transfected with the *MDR1* gene, which encodes Pgp, were seeded on a multiscreen plate (Millipore Corporation, Billerica, MA). After cells formed a confluent layer, the test drug was added to the apical side of the membrane. The drug concentrations in the apical and basolateral media were determined 60 min after drug addition. The ability of a compound to concentrate across the cell barrier to the basolateral side indicates that it is a substrate for transport by Pgp. The permeability coefficient (P_{app}) was calculated as $P_{app} = (dQ/dt)/(C_0 \times A)$, where dQ/dt is the rate of permeation of the drug across the cells, C_0 is the apical donor compartment concentration at time 0, and A is the area of the cell monolayer. The efflux ratio was calculated as $P_{app(B-A)}/P_{app(A-B)}$ from the mean apical to basolateral ($P_{app(A-B)}$) and basolateral to apical ($P_{app(B-A)}$) transport events. Propranolol, a drug that is not a Pgp substrate, was used as a negative control, and prazosin, a known Pgp substrate, was used as a positive control. Cyclosporin A was used as a competitive inhibitor of Pgp-mediated drug transport. An efflux value greater than 2 is an indication that the drug is a substrate for Pgp-dependent efflux.

Immunofluorescence and EC_{50} Calculation. A-10 or HeLa cells were plated on glass coverslips and allowed to adhere for 24 h before the addition of compounds. Eighteen hours after drug addition, cells were fixed with methanol and stained for β-tubulin by indirect immunofluorescence as previously described (Tinley et al.,

2003a). Cells were washed, incubated with 0.1 μg/ml DAPI, and visualized using a Nikon Eclipse 80i fluorescence microscope and NIS Elements software (Nikon, Melville, NY). The EC_{50} for microtubule depolymerization was determined as described previously (Lee et al., 2010).

Flow Cytometry. HeLa cells were treated with drugs for 18 h and then harvested by cell scraping and centrifugation. Cells were resuspended in Krishan's reagent containing propidium iodide (Krishan, 1975), and cell cycle distribution was evaluated on a FACSCalibur flow cytometer (BD Biosciences, San Jose, CA). Propidium iodide intensity was plotted versus the number of events using ModFIt LT 3.0 (Verity Software House, Topsham, ME).

Tubulin Polymerization. The direct effect of CA-4 and ELR510444 on the rate and extent of tubulin polymerization was determined by monitoring the turbidity of purified porcine brain tubulin (Cytoskeleton, Denver, CO) at A_{340}. The reaction was conducted in general tubulin buffer (BST 01–001; Cytoskeleton) with 10% glycerol and 1 mM GTP at 37°C. The final concentration of tubulin in the reaction was 3 mg/ml.

Colchicine Displacement. Colchicine displacement studies evaluate the ability of compounds to compete with colchicine binding to tubulin. Displacement can be measured with radiolabeled colchicine or using flurometric detection (Bhattacharyya and Wolff, 1974; Kang et al., 1990). In this study, fluorometric detection was used to determine the ability of ELR510444 to displace colchicine binding to tubulin. In brief, 2 μM porcine brain tubulin (Cytoskeleton) was incubated alone, with 2 μM colchicine, or with 2 μM colchicine in the presence of 50, 100, or 200 μM ELR510444 in buffer A (0.1 2-(*N*-morpholino)ethanesulfonic acid sodium, pH 6.4, 1 mM EGTA, 0.2 mM EDTA, 0.5 mM $MgCl_2$, and 1 mM GTP). Fluorescence was measured after incubation at 37°C for 2 h using a Horiba Fluoromax-3 spectrofluorometer (Horiba Jobin Yvon, Edison, NJ) at an excitation of 380 nm and emission of 438 nm (Banerjee and Luduena, 1992). The raw fluorescence values were normalized first by subtracting the fluorescence of the buffer and then setting the fluorescence of 2 μM tubulin with 2 μM colchicine to 100%.

In Vivo Antitumor Efficacy. Antitumor effects of ELR510444 were evaluated in a MDA-MB-231 xenograft model. ABT-751, a microtubule-targeting agent with vascular disrupting activity and structural similarity to ELR510444 (Luo et al., 2009), was used as a positive control. ABT-751 was formulated in 0.5% methylcellulose in water, and ELR510444 was formulated in 10% DMSO with 10% Cremophor in water. Female BALB/c nude mice, aged 6 to 7 weeks, were inoculated via subcutaneous injection with MDA-MB-231 cells that had been cultured for 3 to 4 weeks. Each animal received 0.20 ml of cell suspension (0.1 ml of cells + 0.1 ml of Matrigel). Animals were monitored throughout the study period for adverse effects, and body weights were recorded daily. Tumor areas (length × width) were measured twice weekly by using digital calipers throughout the study period, and tumor volumes were calculated based on the following formula: tumor volume = (length × $width^2$)/2. Once tumors reached 150 to 300 mm^3, animals were divided into five groups of 10: vehicle control (10% DMSO with 10% Cremophor in water), ABT-751 (75 mg/kg), and three doses of ELR510444 (3, 6, and 12.5 mg/kg). Drugs were administered orally at the indicated dose once daily for 28 days. Relative change of body weight was calculated based on the following formula: percent relative change of body weight = $(BW_i - BW_0)/BW_0 \times 100\%$, where BW_i is the body weight on the day of dosing, and BW_0 is the body weight on the first day of administration. Tumor growth inhibition was calculated for each group according to the following formula: percent tumor growth inhibition = $[1 - (Ti - T_0)/(Vi - V_0)] \times 100$, where Ti is the tumor volume of treatment group on a specific day, T_0 is the tumor volume of the treatment group on the first day, Vi is the tumor volume of vehicle control group on a specific day, and V_0 is the tumor volume of the vehicle group on the first day of treatment. Single-dose pharmacokinetic studies were performed by liquid chromatography-tandem mass spectrometry of plasma taken from mice at 0 to 8 h after a single oral dose of 25 mg/kg ELR510444. A maximum tolerated dose of 12.5 mg/kg was established during a 7-day study where ELR510444 was dosed orally at 12.5, 25, or 50 mg/kg once a day. No significant body weight loss or change in hematological parameters was observed with the 12.5 mg/kg dose.

Endothelial Cell Morphology Assay. The effects of ELR510444 on endothelial cell morphology were evaluated in 2H-11 tumor endothelial cells (Walter-Yohrling et al., 2004). 2H-11 cells were plated on glass coverslips and allowed to attach and grow for 24 h. Drugs were then added for 1 h, and cells were fixed with paraformaldehyde and permeabilized with Triton X-100. F-Actin and DNA were stained with tetramethylrhodamine B isothiocyanate-conjugated phalloidin (Sigma-Aldrich) and DAPI, respectively, as described previously (Simmons et al., 2009). Images were acquired on a Nikon Eclipse 80 microscope using NIS Elements software.

Results

ELR510444 Causes Inhibition of Cell Proliferation and Overcomes Drug Resistance Mechanisms. ELR510444 (Fig. 1A) inhibited the proliferation of MDA-MB-231 breast cancer cells with an IC_{50} value of 30.9 ± 2.3 nM (Fig. 1, B and D). This low nanomolar potency is consistent with the in vitro potency of other microtubule destabilizers that are used clinically and others in clinical development, including CA-4, which has an IC_{50} value in this cell line of 11.9 ± 1.2 nM (Fig. 1, C and D). The IC_{50} values for ELR510444 in the MDA-MB-435 melanoma cell line and the 2H-11 tumor endothelial cell line were 9.0 ± 0.5 and 11.7 ± 0.4 nM, respectively (Fig. 1D). An EC_{50} for caspase 3/7 induction of 19 nM ELR510444 was observed in the HCT-116 cell line, which has an IC_{50} value of 17 nM, consistent with an apoptotic mechanism of cell death (data not shown).

The ability of ELR510444 to circumvent the two clinically relevant forms of resistance to microtubule-targeted agents, overexpression of Pgp or the βIII isotype of tubulin, was studied. A cell-based assay that evaluates the ability of compounds to be concentrated across a membrane of cells expressing Pgp was used to evaluate whether ELR510444 is a substrate of Pgp. Propranolol, which is not a Pgp substrate, was not concentrated across the confluent monolayer of Pgp-overexpressing cells, as evidenced by an MDR1 efflux ratio of less than 1 (Fig. 1E). In contrast, prazosin, a known Pgp substrate, yielded an efflux ratio of 44.4, which was effectively attenuated upon coincubation with the Pgp inhibitor cyclosporin A (Fig. 1E). ELR510444 was not concentrated across the membrane, as indicated by an efflux ratio of 0.78 in this assay (Fig. 1E). ELR510444 also showed efficacy in the Pgp-overexpressing cell line SK-OV-3/MDR-1-6/6, as demonstrated by a Rr value of 2.3 compared with the parental SK-OV-3 cell line (Fig. 1D). Paclitaxel, a known Pgp substrate, has an Rr value of 1822 in this cell line pair, and CA-4, which is known to circumvent this mode of resistance, has an Rr value of 3.0 (Fig. 1D). These data demonstrate that ELR510444 is not a substrate of the Pgp transporter and thus is expected to retain efficacy in Pgp-expressing tumors.

The ability of ELR510444 to circumvent βIII-tubulin-mediated drug resistance was also evaluated in a pair of isogenic cell lines. ELR510444 had an Rr value of 1.4 in βIII-expressing HeLa cells compared with the parental HeLa cell line (Fig. 1D). This relative resistance value is identical to that obtained with CA-4 in a side-by-side comparison of the two agents (Fig. 1D). In contrast, paclitaxel showed an Rr value of 7.6 in this cell line pair (Fig. 1D). These findings are

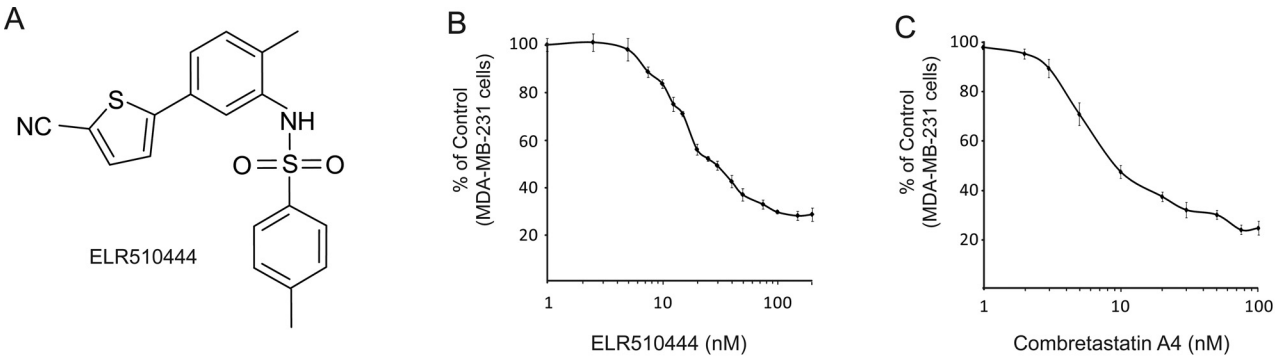

D

	ELR510444 (nM)	CA-4 (nM)	Paclitaxel (nM)
MDA-MB-231	30.9 ± 2.3	11.9 ± 1.2	
MDA-MB-435	9.0 ± 0.5	3.2 ± 0.1	
2H-11	11.7 ± 0.4	4.5 ± 0.5	
HeLa	13.1 ± 1.3	4.4 ± 0.4	1.2 ± 0.1
WTβIII	18.8 ± 0.3	6.3 ± 0.2	9.1 ± 0.5
(Rr)	(1.4)	(1.4)	(7.6)
SK-OV-3	18.4 ± 1.3	5.0 ± 0.7	2.6 ± 0.2
SK-OV-3/MDR-1-6/6	43.0 ± 2.3	14.8 ± 0.6	4,738 ± 135
(Rr)	(2.3)	(3.0)	(1,822)

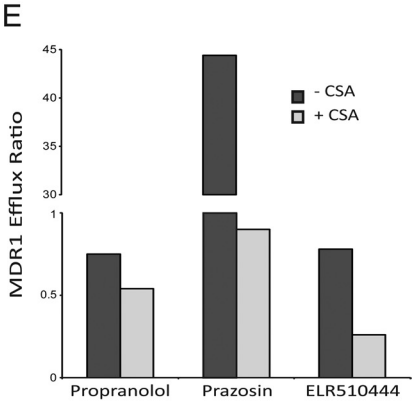

Fig. 1. A, chemical structure of ELR510444. B and C, dose-dependent effects of ELR510444 (B) and CA-4 (C) on the proliferation of the MDA-MB-231 breast cancer cell line. D, the SRB assay was used to determine the IC_{50} values for inhibition of proliferation of MDA-MB-231, MDA-MB-435, 2H-11, HeLa, WTβIII, SK-OV-3, and SK-OV-3/MDR-1-6/6 cells by ELR510444 and CA-4. Rr values were calculated for both sets of drug-resistant cell lines, and paclitaxel was used as a positive control. E, ELR510444 is not a substrate for the Pgp drug efflux pump, as indicated by an efflux ratio less than 2 in the MDR1-MDCK permeability assay. Cyclosporin A (CSA) was used as a competitive inhibitor for Pgp transport.

consistent with previous studies that have demonstrated that all classes of currently approved microtubule-targeting agents, including taxanes, epothilones, and vinca alkaloids, have higher Rr values in this cell line pair than those we observed for ELR510444 (Risinger et al., 2008). Together, these findings demonstrate that ELR510444 can overcome both Pgp- and βIII-mediated drug resistance.

ELR510444 Causes Cellular Microtubule Loss, Mitotic Arrest, and Formation of Multiple Spindles. The effect of ELR510444 on interphase microtubule structures was evaluated in A-10 cells. These cells are valuable for observing drug-induced changes in interphase microtubules because they are relatively large and flat, and they arrest in interphase in response to microtubule-disrupting agents. A range of ELR510444 concentrations was evaluated for effects on microtubules, and the results show that low nanomolar concentrations cause significant loss of interphase microtubules (Fig. 2A), establishing this agent as a microtubule depolymerizer. The concentration required to cause 50% depolymerization of cellular microtubules (EC_{50}) in A-10 cells was determined to be 21 nM (Fig. 2B). For comparison, the EC_{50} value for depolymerization of cellular microtubules in A-10 cells of CA-4 is 7 nM (Lee et al., 2010). It is interesting to note that the concentration of ELR510444 required to cause 50% loss of the cellular microtubules is almost identical to that needed to inhibit proliferation, suggesting that the disruption of microtubules plays a major role in this compound's antiproliferative mechanism of action.

In contrast to A-10 cells, cancer cells arrest in mitosis in the presence of microtubule-disrupting agents, as demonstrated by the accumulation of cells with tetraploid DNA content after treatment with CA-4 or ELR510444 (Fig. 3A). The mitotic spindles that form after treatment with microtubule-targeting agents are abnormal in that they appear as multiple asters instead of a classic bipolar spindle. HeLa cells treated with 25 nM ELR510444 displayed this phenotype of mitotic accumulation with multiple mitotic spindles (Fig. 3B). These spindles differ slightly from those induced by 10 nM CA-4 in that they are more numerous and compact. It is noteworthy that concentrations of ELR510444 or CA-4 only 2 times those shown in Fig. 3B result in a complete loss of visible mitotic spindles as well as any interphase microtubule structures because of their microtubule-depolymerizing properties.

ELR510444 Inhibits the Assembly of Purified Tubulin and Displaces Colchicine. To evaluate whether ELR510444 directly inhibits tubulin polymerization, its effects on the assembly of purified tubulin were evaluated in biochemical assays. The results show that ELR510444 inhibited both the rate and extent of microtubule polymerization in a concentration-dependent manner, with 15% inhibition of polymerization observed at a concentration of 5 μM and 50% inhibition at a concentration of 10 μM (Fig. 4A). In comparison, a 5 μM concentration of CA-4 caused 50% inhibition of tubulin polymerization (Fig. 4A). These data indicate that the microtubule-destabilizing activity of ELR510444 in cells is attributable to a direct effect of the drug on tubulin and that it is slightly less potent than CA-4, consistent with its effects on cellular proliferation and microtubule loss.

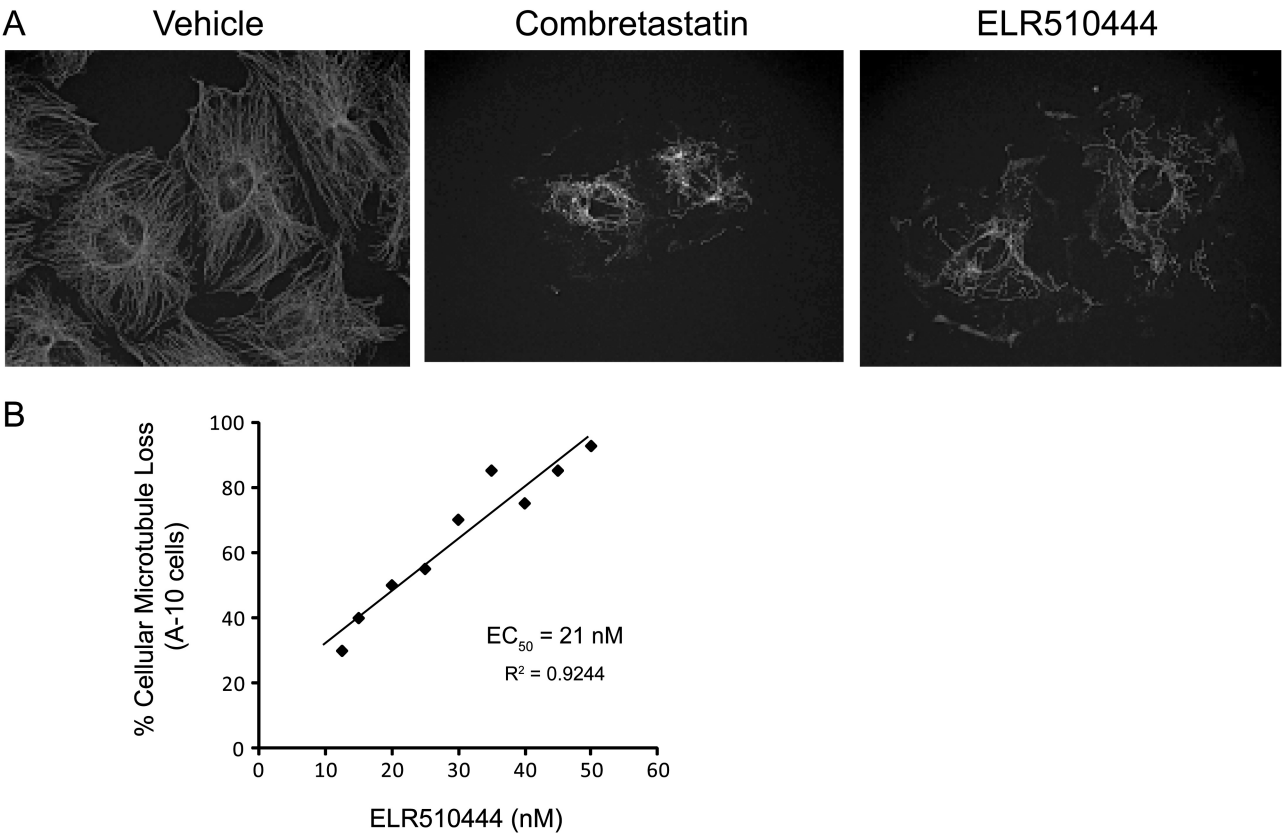

Fig. 2. ELR510444 causes loss of cellular microtubules. A, A-10 cells were treated with vehicle (DMSO), 12.5 nM CA-4, or 50 nM ELR510444 for 18 h. Microtubules were visualized by indirect immunofluorescence for β-tubulin. The loss of cellular microtubules can be seen in CA-4- and ELR510444-treated cells. B, the percent microtubule depolymerization observed at each concentration of ELR510444 was estimated visually, the effects of a range of concentrations were plotted, and the EC_{50} value of 21 nM was calculated from linear regression analysis.

Based on the structural similarity of ELR510444 to ABT-751, which has been shown to bind to the colchicine site on tubulin (Yee et al., 2005), we evaluated whether ELR510444 also binds to the colchicine site. An assay that takes advantage of the fact that colchicine binding to tubulin can be monitored fluorometrically was used (Bhattacharyya and Wolff, 1974). When excited at 380 nm and measured at 438 nm, equimolar concentrations of tubulin and colchicine cause a dramatic increase in fluorescence (Fig. 4B). In contrast, no fluorescence is measured with tubulin alone, colchicine alone, or ELR510444 in the presence or absence of tubulin (Fig. 4B and data not shown, respectively). When ELR510444 was incubated along with tubulin and colchicine, a decrease in fluorescence was observed, indicating that ELR510444 displaces colchicine from tubulin with a maximum displacement of 40% at 100 μM (Fig. 4B). As a negative control, vinblastine (a microtubule destabilizer that binds to the distinct vinca site on tubulin) did not alter the fluorescence observed upon colchicine-tubulin binding, consistent with its known occupancy of a discrete binding site on tubulin (data not shown). Although the displacement of colchicine by ELR510444 is relatively weak compared with many other colchicine site agents, these findings suggest that ELR510444 has some affinity toward the colchicine site on tubulin. Future, more detailed biochemical studies will be required to understand fully the association of ELR510444 with tubulin.

Antitumor Activities of ELR510444. Dose tolerance tests of ELR510444 conducted over a 1-week period were used to identify the maximal tolerated dose of 12.5 mg/kg. Single-dose pharmacokinetic studies indicate that ELR510444 shows a C_{max} of 1.2 μg/ml (~3 μM) 30 min after dosing and a compound half-life ($t_{1/2}$) of approximately 3.6 h (Fig. 5B). The in vivo efficacy of ELR510444 was evaluated in an MDA-MB-231 xenograft model. Once tumors reached 150 to 300 mm^3, three doses of ELR510444 (3, 6, or 12.5 mg/kg) were administered orally once daily for 28 days. ABT-751, a microtubule-depolymerizing agent with vascular disrupting activity and structural similarity to ELR510444 that is currently in phase II clinical trials, was used as a positive control by oral dosing at 75 mg/kg.

ELR510444 caused dose-dependent antitumor effects at doses of 3 and 6 mg/kg, with 6 mg/kg ELR510444 demonstrating antitumor activity comparable with 75 mg/kg ABT-751 (Fig. 5A). No additional antitumor activity was observed at the maximum tolerated dose of 12.5 mg/kg compared with the 6 mg/kg dose, indicating that optimal antitumor effects can be achieved at doses 2-fold lower than the maximum tolerated dose. Therefore, ELR510444 has at least a 2-fold therapeutic window, which is comparable with the therapeutic window achieved in preclinical models of other microtubule-targeting agents used in the clinic, including paclitaxel (Towle et al., 2001). In addition, with these doses of ELR510444, animal body weight was maintained during the first 2 weeks of treatment, and although minor weight loss was observed in the last 2 weeks of treatment, weights never dropped below the initial body weight (data not shown). These results show that daily oral dosing of ELR510444 at 6

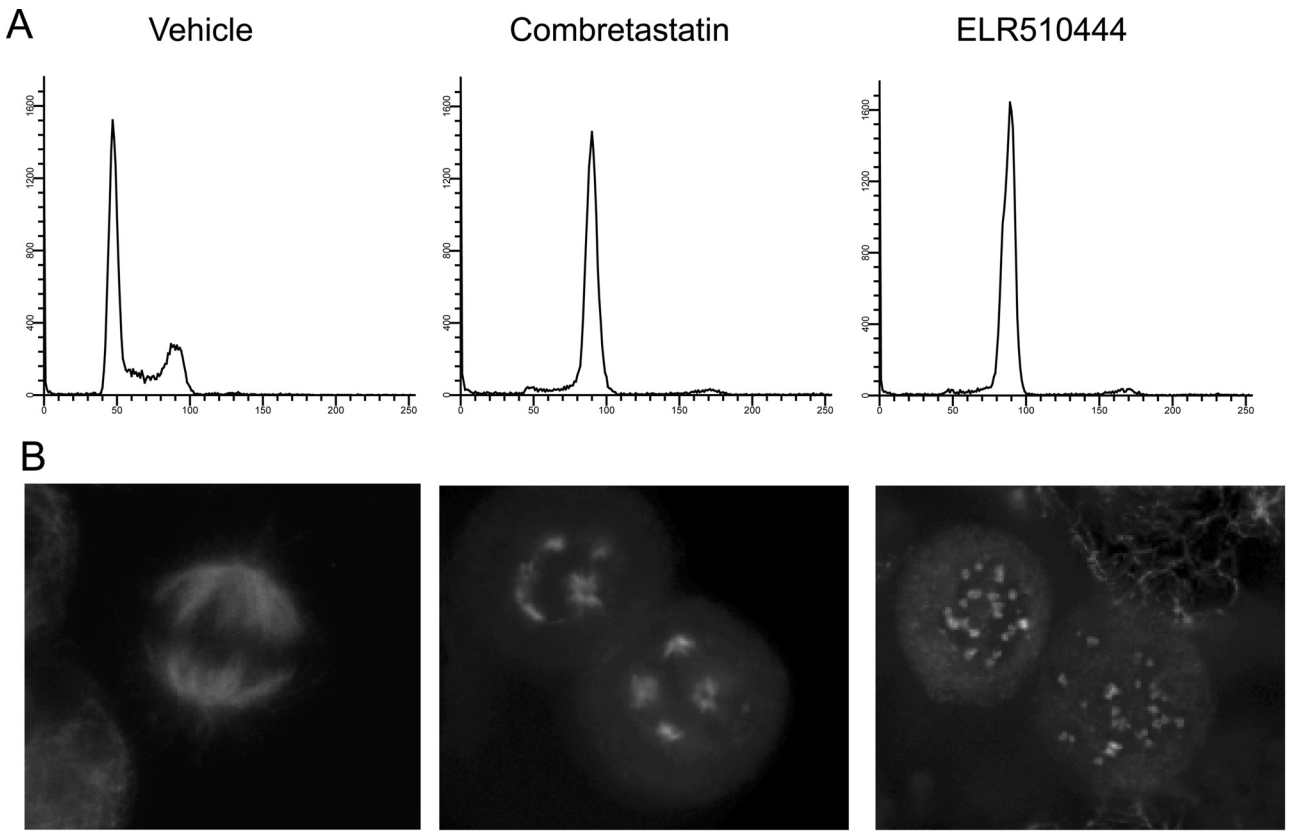

Fig. 3. ELR510444 causes mitotic arrest and aberrant mitotic spindles. HeLa cells were treated with vehicle alone (DMSO), 10 nM CA-4, or 25 nM ELR510444 for 18 h. A, cells were analyzed for cell cycle distribution by propidium iodide staining followed by flow cytometry. B, microtubules were visualized by indirect immunofluorescence.

mg/kg provided significant antitumor efficacy with minimal side effects, as indicated by monitoring body weight changes.

In Vitro Evidence of the Vascular Disrupting Properties of ELR510444. In addition to causing mitotic arrest leading to apoptosis in cancer cells, a subset of microtubule depolymerizers cause rapid destruction of tumor vasculature within 1 h of drug treatment, leading to central tumor necrosis (Tozer et al., 2001). This vascular disrupting activity was first demonstrated with CA-4, and subsequently a number of microtubule depolymerizers have been shown to have this effect. Vascular disrupting effects in vivo have been correlated with rapid changes in the morphology of proliferating endothelial cells in vitro (Luo et al., 2009). Immortalized 2H-11 murine endothelial cells have been proposed as an in vitro model of tumor endothelial cells because they express tumor endothelial cell surface markers and demonstrate the properties of human tumor endothelial cells in vitro (Walter-Yohrling et al., 2004). In function, 2H-11 cells form capillary-like tubules when plated on basement membrane constituents, and they respond like human endothelial cells to antiangiogenic agents. 2H-11 cells were incubated with 30 nM ELR510444 or 3 nM CA-4 for 1 h and fixed, and the actin cytoskeleton was visualized with phalloidin. Within 1 h of ELR510444 or CA-4 treatment, dramatic changes in cellular morphology were observed. Changes included retraction of cell-cell contacts and membrane blebbing (Fig. 6). These effects are identical to those observed after 1 h treatment of proliferating human microvascular endothelial cells with low doses of ABT-751 (Luo et al., 2009). This in vitro finding suggests that ELR510444 has the capability to disrupt the morphology of immature, rapidly dividing tumor endothelial cells at concentrations that are readily achieved in vivo, which likely contributes to the observed antitumor effects of this agent.

Discussion

The ratio between the IC_{50} for inhibition of cellular proliferation and the EC_{50} for inhibition of microtubule polymerization provides valuable information regarding the linkage between an agent's antitumor and microtubule-dependent effects. The EC_{50}/IC_{50} ratio for various other colchicine-binding site agents we have analyzed in the laboratory have shown ratios ranging from 1 to 30, with values near 1 suggesting a tight linkage between microtubule depolymerizing and antiproliferative effects. Higher ratios demonstrate that a drug likely has an additional antiproliferative mechanism in addition to its effects on microtubules, which may lead to unwanted side effects. The near-identical EC_{50} and IC_{50} values of ELR510444 indicate that the antiproliferative and antitumor effects of ELR510444 can be largely attributed to its effect on cellular microtubule dynamics.

The ability of microtubule stabilizers, including the taxanes and epothilones, to initiate the formation of aberrant multipolar mitotic spindles has been well established (Chen and Horwitz, 2002). However, there is some discrepancy with regard to the ability of microtubule-destabilizing agents to cause formation of these abnormal mitotic structures between our findings (Fig. 3B) (Tinley et al., 2003a; Weiderhold et al., 2006) and others (Chen and Horwitz, 2002). From our

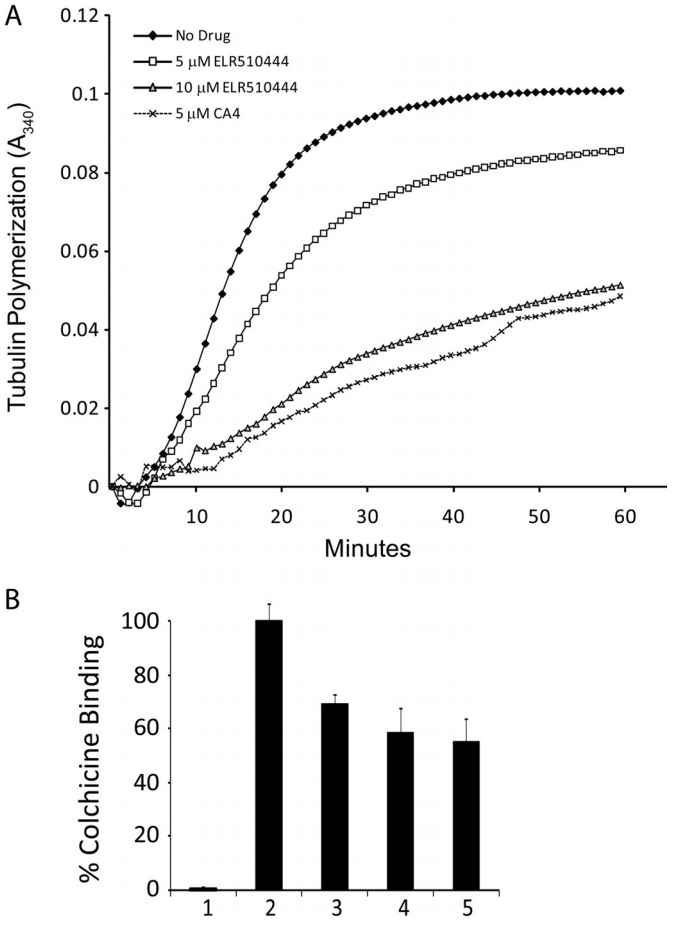

Fig. 4. ELR510444 directly inhibits the polymerization of tubulin. A, purified porcine brain tubulin (Cytoskeleton) was incubated in the presence of vehicle (DMSO), 5 μM CA-4, or 5 or 10 μM ELR510444 in general tubulin buffer with 10% glycerol and 1 mM GTP at 37°C. Tubulin polymerization was monitored by absorbance at 340 nm. B, ELR510444 displaces colchicine from tubulin. The fluorescence of tubulin alone (1); 2 μM colchicine and 2 μM tubulin (2); 2 μM colchicine, 2 μM tubulin, and 50 μM ELR510444 (3); 2 μM colchicine, 2 μM tubulin, and 100 μM ELR510444 (4); and 2 μM colchicine, 2 μM tubulin, and 200 μM ELR510444 (5) was determined. The fluorescence measured with 2 μM colchicine and 2 μM tubulin was set at 100%.

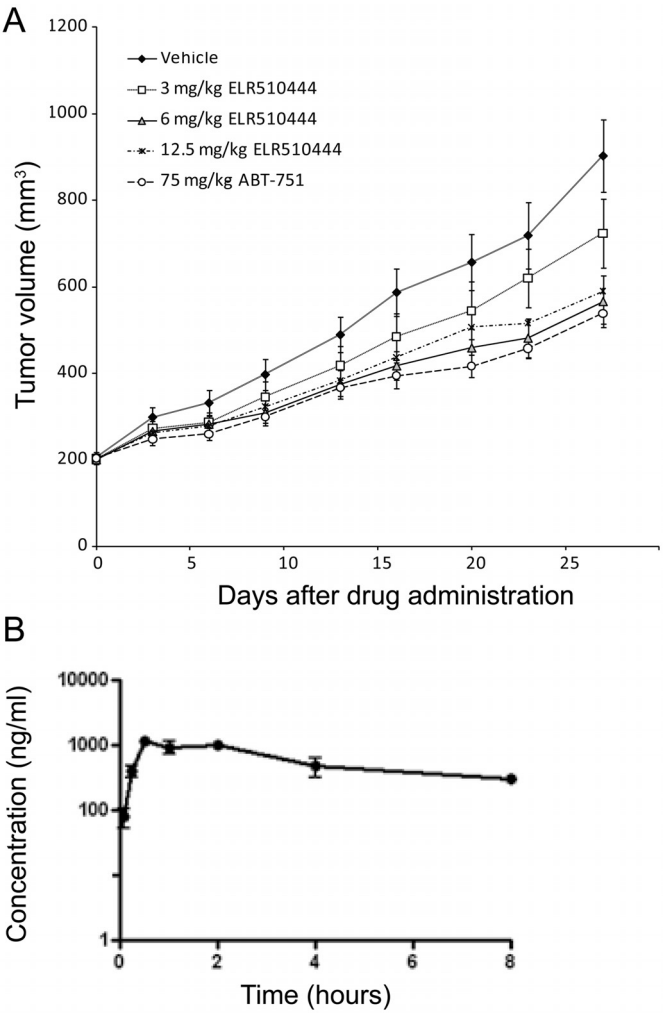

Fig. 5. In vivo antitumor activity of ELR510444. A, dose-dependent antitumor activity was evaluated in the MDA-MB-231 xenograft model with oral dosing of ELR510444 at 3, 6, or 12.5 mg/kg once daily or ABT-751 at 75 mg/kg once daily. B, the plasma compound concentration over time was determined by liquid chromatography-tandem mass spectrometry after a single oral dose of 25 mg/kg.

observations in this study and others, we have found that there is a very small concentration window where multiple spindles can be observed upon treatment of cells with microtubule-destabilizing agents because of the inherent nature of these compounds to inhibit microtubule polymerization and enhance microtubule depolymerization, thus leading ultimately to a loss of all cellular microtubules. For instance, the multiple spindles observed in cells after treatment with CA-4 or ELR510444 in Fig. 3B at 10 and 25 nM, respectively, were not evident when these concentrations were doubled. However, it is worth noting that the size, structure, and number of abnormal mitotic spindles that are formed after treatment with different microtubule-targeting agents often appear to be distinct. Dose-dependent differences in spindle morphologies are also observed in cells treated with different concentrations of the same drug. Therefore, the subtle differences in the structures of the multiple spindles present in CA-4 treated cells compared with ELR510444-treated cells (Fig. 3B) may be due to slight differences in the relative concentrations of each drug evaluated as opposed to inherent differences between the two drugs.

ELR510444 causes cellular microtubule loss and inhibition of cellular proliferation at low nanomolar concentrations, but low micromolar concentrations are required to inhibit the polymerization of purified tubulin. Endogenous cytosolic proteins that play important roles in cellular tubulin polymerization are absent from these assays, which results in the requirement of much higher concentrations of microtubule-targeting drugs than those that affect microtubule dynamics and density in intact cells. In addition, it has been documented using radiolabeled compounds that the concentrations of vinblastine and paclitaxel can be significantly concentrated across the cell membrane. For these reasons, it is not unexpected that the concentration of CA-4 required to inhibit the polymerization of purified tubulin by 50% is 5 μM, which is approximately 500 times greater than the IC_{50} value for inhibition of cell proliferation (Fig. 1C). This is comparable with differences in ELR510444 concentration required to see effects on purified tubulin with the concentration that produced effects in intact cells.

Although it is well established that a subset of microtubule-destabilizing agents can cause vascular disruption, the

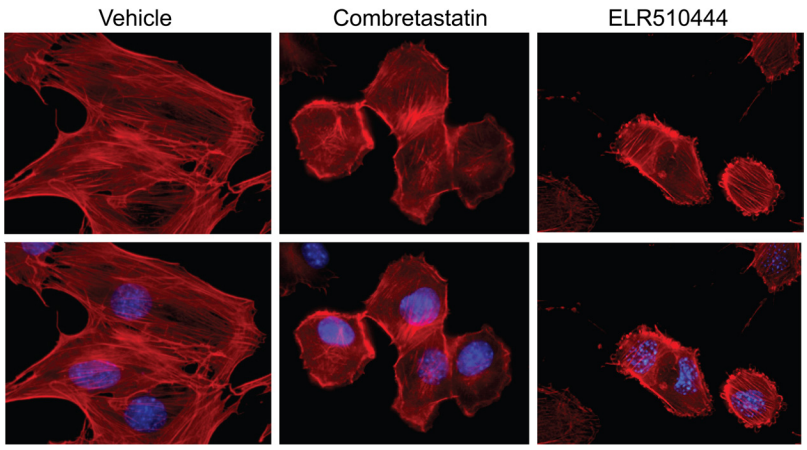

Fig. 6. Effects of ELR510444 on endothelial cell morphology. 2H-11 endothelial cells were treated with vehicle, 3 nM CA-4, or 30 nM ELR510444 for 1 h. The actin cytosketelon (red) and DNA (blue) were visualized by tetramethylrhodamine B isothiocyanate-phalloidin and DAPI staining, respectively.

mechanism by which these agents destroy tumor vasculature without significantly affecting normal vasculature is not known. One well-supported hypothesis is that tumor vasculature is more proliferative, less firmly established, and more disorganized than normal blood vessels with fewer supporting pericytes, leaving it more susceptible to cytoskeletal-induced disruptions in cellular junctions (Hashizume et al., 2000; Baluk et al., 2005). On a more molecular level, the contractibility and membrane blebbing that occurs in endothelial cells after exposure to VDAs, either in vitro or in vivo, has been attributed to Rho-dependent changes in the actin cytoskeleton resulting from microtubule disruption (Kanthou and Tozer, 2002; Yeung et al., 2007). It will be interesting to explore the mechanisms by which some microtubule-destabilizing agents, such as colchicine and the vinca alkaloids, are only able to cause vascular disruption at concentrations approaching their maximum tolerated dose, whereas others, including CA-4, ABT-751, and ELR510444, have this effect at much lower relative concentrations.

Combination treatment of vascular-disrupting agents with classic chemotherapy or radiation has shown promise, but it has become evident that the dosing and timing of each treatment needs to be optimized to effectively eliminate the tumor and prevent regrowth. This multimodality treatment may be recapitulated by treatment with ELR510444 as a single agent because our studies suggest that in addition to its classic cytotoxic effects, ELR510444 has the potential to destroy tumor vasculature (Fig. 6).

Acknowledgments

We thank Richard Ludueña for his assistance with the fluorometric colchicine-displacement assays.

Authorship Contributions

Participated in research design: Risinger, Mooberry, Giles, Westbrook, Mülbaier, Encinas, Lewis, Wawro, Schultes, and Janssen.

Conducted experiments: Risinger, Westbrook, and Wawro.

Contributed new reagents or analytic tools: Mülbaier and Encinas.

Performed data analysis: Risinger, Mooberry, Westbrook, and Wawro.

Wrote or contributed to the writing of the manuscript: Risinger, Mooberry, Giles, Westbrook, Mülbaier, Encinas, Lewis, Wawro, Schultes, and Janssen.

References

Baluk P, Hashizume H, and McDonald DM (2005) Cellular abnormalities of blood vessels as targets in cancer. *Curr Opin Genet Dev* **15:**102–111.

Banerjee A and Luduena RF (1992) Kinetics of colchicine binding to purified beta-tubulin isotypes from bovine brain. *J Biol Chem* **267:**13335–13339.

Bhattacharyya B and Wolff J (1974) Promotion of fluorescence upon binding of colchicine to tubulin. *Proc Natl Acad Sci USA* **71:**2627–2631.

Chen JG and Horwitz SB (2002) Differential mitotic responses to microtubule-stabilizing and -destabilizing drugs. *Cancer Res* **62:**1935–1938.

Chiou JF, Liang JA, Hsu WH, Wang JJ, Ho ST, and Kao A (2003) Comparing the relationship of Taxol-based chemotherapy response with P-glycoprotein and lung resistance-related protein expression in non-small cell lung cancer. *Lung* **181:**267–273.

Fojo T and Menefee M (2007) Mechanisms of multidrug resistance: the potential role of microtubule-stabilizing agents. *Ann Oncol* **18 (Suppl 5):**v3–v8.

Gridelli C, Rossi A, Maione P, Rossi E, Castaldo V, Sacco PC, and Colantuoni G (2009) Vascular disrupting agents: a novel mechanism of action in the battle against non-small cell lung cancer. *Oncologist* **14:**612–620.

Hashizume H, Baluk P, Morikawa S, McLean JW, Thurston G, Roberge S, Jain RK, and McDonald DM (2000) Openings between defective endothelial cells explain tumor vessel leakiness. *Am J Pathol* **156:**1363–1380.

Horsman MR and Siemann DW (2006) Pathophysiologic effects of vascular-targeting agents and the implications for combination with conventional therapies. *Cancer Res* **66:**11520–11539.

Joe PA, Banerjee A, and Ludueña RF (2008) The roles of cys124 and ser239 in the functional properties of human betaIII tubulin. *Cell Motil Cytoskeleton* **65:**476–486.

Jordan MA and Kamath K (2007) How do microtubule-targeted drugs work? An overview. *Curr Cancer Drug Targets* **7:**730–742.

Kang GJ, Getahun Z, Muzaffar A, Brossi A, and Hamel E (1990) N-acetylcolchinol O-methyl ether and thiocolchicine, potent analogs of colchicine modified in the C ring. Evaluation of the mechanistic basis for their enhanced biological properties. *J Biol Chem* **265:**10255–10259.

Kanthou C and Tozer GM (2002) The tumor vascular targeting agent combretastatin A-4-phosphate induces reorganization of the actin cytoskeleton and early membrane blebbing in human endothelial cells. *Blood* **99:**2060–2069.

Kanthou C and Tozer GM (2009) Microtubule depolymerizing vascular disrupting agents: novel therapeutic agents for oncology and other pathologies. *Int J Exp Pathol* **90:**284–294.

Krishan A (1975) Rapid flow cytofluorometric analysis of mammalian cell cycle by propidium iodide staining. *J Cell Biol* **66:**188–193.

Lee L, Robb LM, Lee M, Davis R, Mackay H, Chavda S, Babu B, O'Brien EL, Risinger AL, Mooberry SL, et al. (2010) Design, synthesis, and biological evaluations of 2,5-diaryl-2,3-dihydro-1,3,4-oxadiazoline analogs of combretastatin-A4. *J Med Chem* **53:**325–334.

Leonard GD, Fojo T, and Bates SE (2003) The role of ABC transporters in clinical practice. *Oncologist* **8:**411–424.

Luo Y, Hradil VP, Frost DJ, Rosenberg SH, Gordon GB, Morgan SJ, Gagne GD, Cox BF, Tahir SK, and Fox GB (2009) ABT-751, a novel tubulin-binding agent, decreases tumor perfusion and disrupts tumor vasculature. *Anticancer Drugs* **20:**483–492.

Pasquier E, Sinnappan S, Munoz MA, and Kavallaris M (2010) ENMD-1198, a new analogue of 2-methoxyestradiol, displays both antiangiogenic and vascular-disrupting properties. *Mol Cancer Ther* **9:**1408–1418.

Rajkumar SV, Richardson PG, Lacy MQ, Dispenzieri A, Greipp PR, Witzig TE, Schlossman R, Sidor CF, Anderson KC, and Gertz MA (2007) Novel therapy with 2-methoxyestradiol for the treatment of relapsed and plateau phase multiple myeloma. *Clin Cancer Res* **13:**6162–6167.

Risinger AL, Jackson EM, Polin LA, Helms GL, LeBoeuf DA, Joe PA, Hopper-Borge E, Ludueña RF, Kruh GD, and Mooberry SL (2008) The taccalonolides: microtubule stabilizers that circumvent clinically relevant taxane resistance mechanisms. *Cancer Res* **68:**8881–8888.

Sève P and Dumontet C (2008) Is class III beta-tubulin a predictive factor in patients receiving tubulin-binding agents? *Lancet Oncol* **9:**168–175.

Simmons TL, Nogle LM, Media J, Valeriote FA, Mooberry SL, and Gerwick WH (2009) Desmethoxymajusculamide C, a cyanobacterial depsipeptide with potent cytotoxicity in both cyclic and ring-opened forms. *J Nat Prod* **72:**1011–1016.

Skehan P, Storeng R, Scudiero D, Monks A, McMahon J, Vistica D, Warren JT,

Bokesch H, Kenney S, and Boyd MR (1990) New colorimetric cytotoxicity assay for anticancer-drug screening. *J Natl Cancer Inst* **82:**1107–1112.
Tinley TL, Leal RM, Randall-Hlubek DA, Cessac JW, Wilkens LR, Rao PN, and Mooberry SL (2003a) Novel 2-methoxyestradiol analogues with antitumor activity. *Cancer Res* **63:**1538–1549.
Tinley TL, Randall-Hlubek DA, Leal RM, Jackson EM, Cessac JW, Quada JC Jr, Hemscheidt TK, and Mooberry SL (2003b) Taccalonolides E and A: plant-derived steroids with microtubule-stabilizing activity. *Cancer Res* **63:**3211–3220.
Towle MJ, Salvato KA, Budrow J, Wels BF, Kuznetsov G, Aalfs KK, Welsh S, Zheng W, Seletsk BM, Palme MH, et al. (2001) In vitro and in vivo anticancer activities of synthetic macrocyclic ketone analogues of halichondrin B. *Cancer Res* **61:**1013–1021.
Tozer GM, Prise VE, Wilson J, Cemazar M, Shan S, Dewhirst MW, Barber PR, Vojnovic B, and Chaplin DJ (2001) Mechanisms associated with tumor vascular shut-down induced by combretastatin A-4 phosphate: intravital microscopy and measurement of vascular permeability. *Cancer Res* **61:**6413–6422.
Trock BJ, Leonessa F, and Clarke R (1997) Multidrug resistance in breast cancer: a meta-analysis of MDR1/gp170 expression and its possible functional significance. *J Natl Cancer Inst* **89:**917–931.
Walter-Yohrling J, Morgenbesser S, Rouleau C, Bagley R, Callahan M, Weber W, and Teicher BA (2004) Murine endothelial cell lines as models of tumor endothelial cells. *Clin Cancer Res* **10:**2179–2189.
Weiderhold KN, Randall-Hlubek DA, Polin LA, Hamel E, and Mooberry SL (2006) CB694, a novel antimitotic with antitumor activities. *Int J Cancer* **118:**1032–1040.
Yee KW, Hagey A, Verstovsek S, Cortes J, Garcia-Manero G, O'Brien SM, Faderl S, Thomas D, Wierda W, Kornblau S, et al. (2005) Phase 1 study of ABT-751, a novel microtubule inhibitor, in patients with refractory hematologic malignancies. *Clin Cancer Res* **11:**6615–6624.
Yeung SC, She M, Yang H, Pan J, Sun L, and Chaplin D (2007) Combination chemotherapy including combretastatin A4 phosphate and paclitaxel is effective against anaplastic thyroid cancer in a nude mouse xenograft model. *J Clin Endocrinol Metab* **92:**2902–2909.
Yoshimatsu K, Yamaguchi A, Yoshino H, Koyanagi N, and Kitoh K (1997) Mechanism of action of E7010, an orally active sulfonamide antitumor agent: inhibition of mitosis by binding to the colchicine site of tubulin. *Cancer Res* **57:**3208–3213.

Address correspondence to: Dr. Susan L. Mooberry, University of Texas Health Science Center at San Antonio, 7703 Floyd Curl Dr., San Antonio, TX 78229. E-mail: mooberry@uthscsa.edu